Electrophoresis

WILEY-VCH

ELECTROPHORESIS

RESEARCH ARTICLE OPEN ACCESS

Surfactant-Based Polymer Microchip Electrophoresis of Ciprofloxacin Hydrochloride Monohydrate in Unfiltered Milk With Fluorescence Detection

Camille A. Leclerc[1] | Christopher G. D. Ty[1] | Sean S. Worthington[1] | Malley B. Richardson[1] | Abdulla K. AlSawalhi[1] | Larry Wood[2] | Khalid Moomand[3] | Christopher M. Collier[1]

[1]Collier Research Group, School of Engineering, The University of British Columbia, Kelowna, British Columbia, Canada | [2]CG Wellington, Drayton, Ontario, Canada | [3]Agrisan Specialty Chemical and Pharmaceutical, Arthur, Ontario, Canada

Correspondence: Christopher M. Collier (christopher.collier@ubc.ca)

Received: 25 April 2024 | **Accepted:** 15 January 2025

Funding: This work was funded through the Natural Sciences and Engineering Research Council of Canada NSERC Discovery Grant program (RGPIN-2023-04202) and NSERC Alliance Grant program (ALLRP 570519–2021). This is an NSERC Alliance grant that involves an industry partner Agrisan Specialty Chemical and Pharmaceutical (which is a subsidiary of CG Wellington).

Keywords: antibiotic detection | microchip electrophoresis | milk | PMMA

ABSTRACT

This work describes a cross-shaped PMMA ME system capable of detecting ciprofloxacin hydrochloride monohydrate (CPFH) in unfiltered milk samples. The cross-shaped PMMA ME system utilizes a BGE consisting primarily of the surface-active agent SDS to solubilize milk fat and improve the zeta potential of the PMMA microchannel surface. A theoretical lumped-element circuit model for cross-shaped ME is introduced in this work to calculate the migration time of CPFH. This manuscript improves the capabilities of PMMA-based ME for CPFH in milk using an SDS-based BGE. The presented ME system has a faster migration time, higher mean output voltage, and thinner full-width at half-maximum than previously reported dairy-based biosensor systems. Most notably, the migration time of the new system is under 10 min, being the time associated with the milking of cattle. The system is also found to be able to detect the presence of milk fat. Discussion is included of potential future integration with existing high-sensitivity methodologies to place the overall ME system's limit of detection below an established target. To the authors' knowledge, this is the first reported account of a PMMA ME system capable of detecting CPFH in unfiltered milk.

1 | Introduction

Advancements made in the 20th century to miniaturize electrical technologies resulted in the formation of microfluidics. Manz et al. melded microfluidics and CE together to form ME, an important contribution for the separation of analytes in a compact microchip device [1]. Microchip electrophoresis is an effective electrophoretic system that requires only minute reagent and sample volumes, yields rapid results, and requires minimal power for operation [2]. Given these advantageous properties, ME systems are currently being investigated for applications in clinical diagnostics [3], biochemical analyses [4], forensic analyses [5], environmental monitoring [6], pharmaceutical analyses [7], and for food quality assessment [2, 8]. Traditionally, ME systems were made of silica to resemble the separation mechanisms observed in CE. However, within the last decade, polymer-based ME

Abbreviations: 1%, one percent milk; CPFH, ciprofloxacin hydrochloride monohydrate; DR, drain well; EDL, electric double layer; FWHM, full-width at half-maximum; HVS, high-voltage sequencer; PMMA, polymethyl-methacrylate; SA, sample well; SM, skim milk; SO, source well; UV, ultraviolet; WA, waste well; WM, whole milk.

systems have emerged. The shift toward the use of a polymer substrate for ME (as opposed to a silica substrate) is due to its economical microfabrication, ability to incorporate unique designs and features, optical transparency, and high durability [2, 9–12]. However, polymer-based ME systems are much less explored than their silica counterparts.

An emerging application of interest for ME systems is antibiotic detection in dairy milk [13, 14]. This is motivated by the important role that antibiotics have in the dairy industry for the treatment of bacterial infections [14–16]. Livestock can be administered one or more antibiotics to combat illnesses [17], and consequently, milk can become contaminated. This contamination of milk poses adverse effects to consumers and to the dairy industry [15–18]. Common antibiotics used in the dairy industry are fluoroquinolones such as ciprofloxacin hydrochloride monohydrate (CPFH) and have been detected through ME, albeit with long (greater than 10 min) analysis times [16, 19]. Currently, there are limited portable methods available to test for antibiotics in milk. Common portable tests for antibiotics include Delvotest and the Charm rapid one-step assay [14, 20]. However, they are semi-quantitative and struggle to distinguish antibiotics within the same group [14, 20] and are prone to human error [20]. Good quantification of antibiotic concentrations is important for antibiotic regulation [15, 21] and prevents farmers from discarding batches of milk [15, 22], which leads to a significant loss of profits [23].

An advantage of these current portable methods for detecting antibiotics in milk is the ability to detect analytes without pretreating the milk [14], and this is in contrast to ME systems. A barrier to ME technologies being used on farms is twofold. Such a system would need to be made adequately fast, for example, with an analysis time less than 10 min [14], which is the maximum time to milk a cow in a modern dairy parlor [14, 24]. These all must be balanced while still maintaining portability [14] and suitably low-voltage operation [25]. The development of such an ME system may allow on-farm measurements and sensing of antibiotics in milk.

The above-stated desirable attributes for an ME system can be elaborated upon. For the context of this paper, a low-voltage ME system will be defined as an ME system that supplies less than or equal to 500 V DC to its electrodes, in comparison to other CE and ME dairy systems with voltages commonly exceeding 2 kV [8], which pose greater safety and logistical challenges. Although logistically challenging, these high voltages are able to make some CE and ME systems yield migration times (t_m) of 5 min or less [2, 26–30]. However, it is desirable to produce a system with both a short t_m (< 10 min) and low voltage (< 500 V).

An additional challenge in developing ME systems for on-farm applications is the current necessity for sample pretreatment to remove unwanted constituents. Commonly in literature, CE and ME milk samples are centrifuged, filtered, and chemically treated [2, 8, 31, 32]. These sample pretreatments alone typically require two to three times the maximum time to milk a cow and require chemicals not typically found on-farm. For most cases, these sample pretreatments are used to remove fat content within the milk sample, as it can obstruct the capillaries (i.e., microchannels) during electrophoresis operations [31]. As raw milk naturally contains fat, achieving an ME or CE system capable of operating with virtually no sample pretreatment is integral to ensure analytes can be detected, and EOF conditions will not be compromised by microchannel clogging. Therefore, surfactants are explored in this work to alleviate this issue.

In this work, we improve upon previously reported dairy-based ME systems. We significantly improve t_m of CPFH through the use of a PMMA microchip and an SDS-based BGE. We avoid sample pretreatment of fatty unfiltered milk through the use of SDS. We are able to meet the target t_m of 10 min and sample pretreatment avoidance with a low voltage (< 500 V) system. This is because SDS significantly improves the EOF of PMMA microchips [9, 10] and solubilizes nonpolar molecules such as fats [33, 34], and because CPFH does not interact with the SDS micelles for pH ranges of 5.0–7.0 [35]. The reported ME device is capable of detecting (but not quantifying) the milk fat. Compared to previously published ME systems [25, 36], the t_m for the presented system is approximately twice as fast. An additional contribution of this work is the improved theory from using a cross-channel lumped-element model. With this introduced model, we are able to better estimate the applied electric fields when compared to the capillary parallel plate model. These results demonstrate that low-voltage polymer-based ME systems are a promising technology for on-farm quinolone antibiotic detection.

2 | Materials and Methods

2.1 | Materials and Equipment

2.1.1 | Sample and Reagents

The skim milk (SM), one percent milk (1%), and whole milk (WM) acquired for this work were of the Dairyland brand (Saputo Inc, Saint-Laurent, Canada), purchased from a local supermarket and used as is. The CPFH used for this work had a molecular weight of 385.82 g/mol (LKT Laboratories Inc, St. Paul, USA). Ultrapure water with a resistivity of 18 MΩcm was acquired as needed using a PURELAB Ultra Water Purification System (ELGA LabWater North America, Woodridge, USA). Anhydrous sodium hydroxide (NaOH) pellets with a molecular weight of 40 g/mol were acquired (LabChem Inc, Zelienople, USA) and used in solution to clean and condition the microchips. The anhydrous NaOH was dissolved in ultrapure water down to a 1 M stock. The following chemicals were used for the BGE: A 0.5 M, 6.0 pH citrate buffer was used as is (Thermo Fisher Scientific, Surrey, Canada). A stock of 10% (1.7 M) acetic acid solution was used as is (Reinhart Foods Ltd, Surrey, Canada). Anhydrous SDS, molecular biology grade 99% with a molecular weight of 288.38 g/mol (Thermo Fisher Scientific, Surrey, Canada), was dissolved in ultrapure water to a 0.1 M stock.

2.1.2 | Materials and Hardware

Platinum electrodes of 584 μm diameter and 99.95% purity were acquired for this work (LabSmith, Livermore, USA). A high-voltage sequencer (HVS), Keithley 2290-5 high-voltage power

supply (Tektronix, Beaverton, USA), ultraviolet (UV) LED circuit board, photodiode (SFH 2440, Osram, Munich, Germany) mounted to a 10^9-gain transimpedance amplifier system, and band-pass filter (86-339, Edmund Optics, Barrington, USA) were used. Although both the ME and fluorescence systems are shown to have high specificity (i.e., minimal occurrence of false positives) [37–41], the SFH 2440 photodiode and 86–339 band-pass filter were chosen carefully to prevent the measurement of the fluorescence emission of milk proteins (340 nm) from the 280 nm UV LED [42]. The SFH 2440 photodiode was chosen as it has a responsivity between 400 and 700 nm, while the 86–339 bandpass (440 ± 20 nm) was chosen to ensure only the CPFH signal is recorded. It can also be noted that the use and implementation of nanomaterials (such as quantum dots) and masking agents within background electrolyte additives (such as surfactants) has reduced the occurrence of false positives in electrophoretic systems [43–45] or by incorporating additional detection schemes [46, 47].

The voltage potentials applied to the wells during the separation phase were measured with a Fluke 115 multimeter (Fluke, Everett, USA). A NI 6343 (National Instruments, Austin, USA) analog-to-digital data acquisition module was used to measure the output of the photodiode located at the detection site of the microchip. A UV LED was chosen for the presented ME system, being the LTPL-G35UV275GC-E (LITE-ON Technology Corporation, New Taipei City, Taiwan) model. This model offers 10 mW of spectral flux at 280 nm and sufficient thermal performance. The optical emission spectra of the UV LED used is shown in Figure S1. The transimpedance amplifier, HVS, and UV LED were powered by a B&K Precision Triple Output DC Power Supply 1760A (Tektronix, Beaverton, USA). The Fluidic 106 PMMA cross-shaped microchips with 75 µm depth by 75 µm width microchannels were used (microfluidic ChipShop, Jena, Germany). For thorough cleaning of the microchips, a Branson 2800 ultrasonic cleaner was used (Emerson Electric Co, St. Louis, USA). To fill the microchannels with aqueous solutions, a vacuum was applied at the desired well using a custom-built vacuum system with a model 2QL56C17F478A (discontinued) vacuum pump (Marathon Electric, Wausau, USA). The mass of all anhydrous reagents was measured with a Nimbus NBL 214e 0.1 mg readability precision scale (Adam Equipment Company, Kingston, UK). For pH measurements, a pH 150 bench meter was used (Oakton Instruments, South Carolina, USA). A handheld conductivity meter was used to measure the bulk conductivity of solutions when needed (LAWNFUL, California, USA). A schematic of the ME device is shown in Figure 1A.

2.2 | Experimental Procedure

The photodiode, HVS, and UV LED circuitry were allowed to warm up with the voltage configurations shown in Table S1 prior to any experiments. A thorough methodology for sample and BGE preparation, microchip conditioning, upkeep, and storage is found in Section B of the Supporting Information. Once the microchip has been conditioned, the source well (SO), waste well (WA), and drain well (DR) reservoirs, are filled with 25 µL of BGE, and the sample well (SA) reservoir is filled with 20 µL of BGE. The microchip was then placed under the microscope

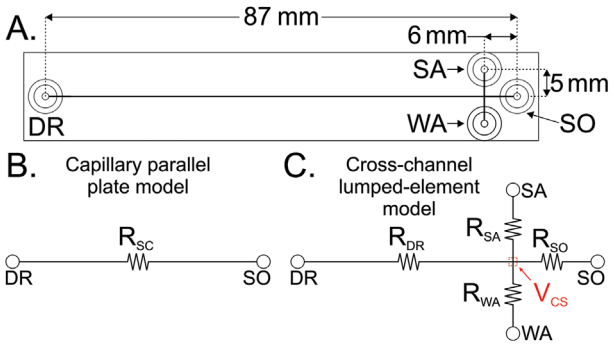

FIGURE 1 | (A) The top view of the schematic is shown for the PMMA microchip used for all experiments with lengths of the microchannels defined and labels SA, SO, WA, and DR to identify the sample, source, waste, and drain wells, respectively. (B) A circuit resistor model is shown of a capillary parallel plate model. (C) Circuit resistor model of the cross-channel lumped-element model is introduced with the voltage at the cross section (V_{CS}) of the microchannels highlighted in red.

stage to ensure the wells and cross-section of the microchip were not contaminated with fibers. The microchip was then carefully placed in an enclosure. The high-voltage power supply is then applied at 500 V. The electrodes located at the SA, SO, DR, and WA were set to 0, 0, 0, and 400 V with the HVS. This configuration ensures no milk sample passively diffuses through the microchannels prior to the injection and separation steps. A 5-µL sample of milk was then injected into the SA reservoir, the electrodes were placed into the reservoirs, and the NI 6343 was actuated to record through a continuous data stream mode of 200 Hz. The SA, SO, DR, and WA electrodes were then actuated using the HVS to the injection configuration (500, 400, 500, and 0 V, respectively) for 30 s. The SA, SO, DR, and WA electrodes were then set to the separation configuration of 250, 500, 0, and 250 V with the HVS. Once the experiment is completed, the NI 6343 as well as the electrodes and high-voltage power supply were turned off, and the microchip was removed from the enclosure and cleaned for another trial or for storage. Snapshots of an ME experiment video submitted as Supporting Information, which follows the voltage potential configurations mentioned above, are shown in Figure 2.

3 | Theory

3.1 | Equations to Calculate Migration Time

For an infinitely thin electric double layer (EDL), the Helmholtz–Smoluchowski expression can be used to quantify EOF mobility (μ_{EO}) and is given by

$$\mu_{EO} = -\frac{\varepsilon_0 \varepsilon_r \zeta_0}{\eta}, \tag{1}$$

where ε_0 is the free space permittivity (8.854×10^{-12} F/m), ε_r is the relative permittivity of the bulk BGE solution, ζ_0 is the zeta potential at the microchannel surface, and η is the viscosity of the bulk BGE solution [10]. The negative sign determines the direction of conventional EOF flow to be cathodic under the presence of an electric field. The electrophoretic mobility (μ_{EP}) is

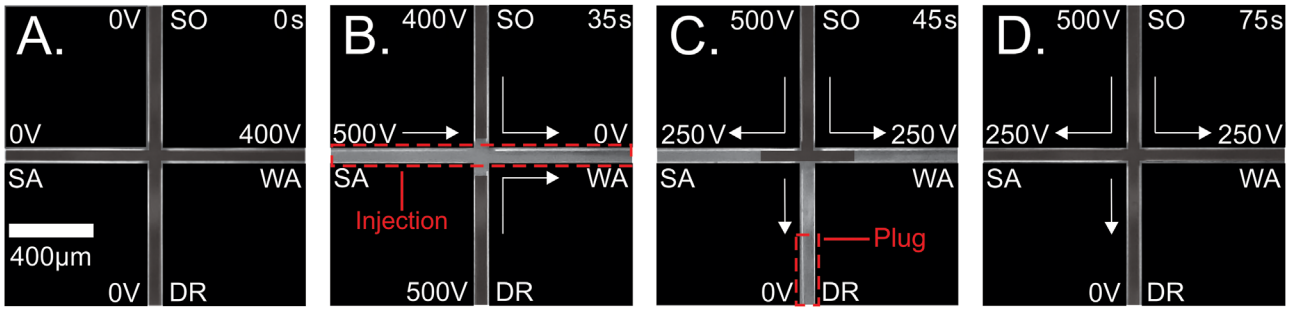

FIGURE 2 | Snippets are shown of the ME experiment video provided in the supporting information, where image (A) shows the microchip prior to the injection voltage configuration. Image (B) shows the microchip after 35 s of recording, where the milk flowing due to the injection configuration is highlighted with the dashed red box. Image (C) is the microchip after 45 s of recording, where the red box highlights the sample plug. Image (D) is the microchip after 75 s of recording. The microchip here is undergoing separation, but no milk is remaining within the microchannels. A color filter is applied to the microchannels containing the BGE to remove visual glare from the microscope and improve contrast. The white arrows indicate the EOF flow within the microchannels once the injection and separation voltages are applied.

given by

$$\mu_{\mathrm{EP}} = \frac{qe}{6\pi\eta r}, \tag{2}$$

where q is the single-molecule net charge of the analyte in the aqueous milieu of the sample, e is the elementary charge (1.602×10^{-19} C), η is the viscosity of the bulk BGE, and r is the hydrodynamic radius of the analyte [48]. The direction of electrophoresis flow is defined by the net charge of the analyte. If the analyte being separated is cationic, the electrophoresis separation will be toward the cathode; an anionic analyte will separate toward the anode.

Upon the presence of an electric field (E), the total velocity (ν_{tot}) of an analyte traveling in a microchannel is given by

$$\nu_{\mathrm{tot}} = (\mu_{\mathrm{EO}} + \mu_{\mathrm{EP}})\, E, \tag{3}$$

where E is the electric field across the separation channel [25]. In this work, the ν_{tot} necessary to attain $t_m < 10$ min is made feasible by improving the ζ_0 of the PMMA microchip with SDS. The use of SDS on PMMA microchips can improve the EOF by over 200% [10]. The value for E can be approximated with

$$E = \frac{\Delta V}{L}, \tag{4}$$

where ΔV is the difference between the voltage potentials applied across the separation channel, and L is the total length of the microchannel that separates the voltage potentials applied to the separation channel [10, 49, 50]. From Equation (3), t_m is given by

$$t_m = \frac{l_d}{\upsilon_{\mathrm{tot}}}, \tag{5}$$

where l_d is the distance from the microchip cross-section to the detection site. The l_d was measured to be 67.5 mm with an electronic caliper. With Equation (5), theoretical computations for the t_m can be made once the appropriate variables from Equations (1)–(5) are found. The values for ε_r, ζ_0, η, q, and r used for this work are 75.5, −85 mV, 1 mPa•s, −0.752, and 0.65 nm, respectively. Further justification for the ε_r, ζ_0, η, q, and r values used is found in Section C of the Supporting Information and summarized in Table S2. Substituting in the necessary values for Equation (1), μ_{EO} was computed to be 5.68×10^{-2} mm^2/V•s, which agrees well with the literature [10]. This μ_{EO} allows the presented ME system's t_m of CPFH to be below 10 min while using low (< 500 V) voltage. From Equation (2), the μ_{EP} was estimated to be -9.81×10^{-3} mm^2/V•s. The following section will define the equations governing the expected electromigration current and Debye length of the EDL—necessary to compute the t_m of the presented PMMA ME system.

3.2 | Lumped Circuit Models

3.2.1 | Electromigration Current and Debye Length

For the analysis of the capillary parallel-plate model and cross-shaped lumped-element model depicted in Figure 1B,C, it is assumed that the current within the ME system is proportional to the bulk conductivity (i.e., ion concentration) of the BGE and that the contribution of the conductance found at the surface of the microchannel due to the EDL is negligible [10]. In addition, due to the reservoirs of each well containing excess BGE, and that the BGE in the reservoirs is replaced after every experiment, ion depletion and consequential buffer mismatch are assumed to be negligible during ME operation [50, 51]. The current (I) in such a system can be modeled with Ohm's Law,

$$I = \sigma A_c E, \tag{6}$$

where σ is the bulk conductivity of the BGE, A_c is the cross-sectional area of the microchannel, and E is the electric field defined from Equation (4) [10, 50]. The thickness of the EDL present on a flat planar surface—such as a microchannel—can be quantified with the Debye length (κ^{-1}) and compared to the radius of the microchannel to determine the negligibility of the EDL [10]. For BGEs with water as the majority of the solvent and electrolytes as their solutes, where the valency between the electrolyte species is asymmetrical, the κ^{-1} for a flat planar surface

is given by

$$\kappa^{-1} = 4.30 \times 10^{-10} \left(\sum_{i=1}^{N} z_i^2 M_i \right)^{-1/2}, \quad (7)$$

where z_i and M_i are the respective valency and molarity of the i^{th} electrolyte species within the BGE [52]. As the BGE used in this work consists of 50 mM SDS, 5 mM citrate buffer, and 2 mM acetic acid, κ^{-1} of the EDL is estimated to be 1.39 nm, which agrees well with the literature for an asymmetrical BGE [52]. Literature reports that if $a \gg \kappa^{-1}$, where a is the microchannel radius, the contribution of the EDL to the bulk σ of the BGE is negligible [10, 52]. As $a = 37.5$ μm for the microchannels of the PMMA microchips used in the presented work, the EDL is deemed to be approximated as infinitely thin and negligible to the bulk σ of the BGE. Therefore, Equation (6) sufficiently describes the electromigration current within the microchip for this work, and the use of Equation (1) to determine the μ_{EO} of the PMMA ME system is validated [10]. This shows that the use of a 50 mM SDS-based BGE provides sufficient EDL characteristics within a PMMA microchip to attain $t_m < 10$ min at low voltage. The following subsections will define the theoretical t_m of CPFH for the capillary parallel-plate model (Figure 1B) and cross-shaped lumped-element model (Figure 1C).

3.2.2 | Capillary Parallel-Plate Model

For the capillary parallel-plate model depicted in Figure 1B, the L value is 87 mm as seen in Figure 1A. Regarding the ΔV used to define E with Equation (4), the authors would like to note that although the voltage potentials for the SA, SO, DR, and WA were set with the HVS as 250, 500, 0, and 250 V for the separation process for all ME experiments, the measured voltage potentials were 230, 400, 3, and 230 V, respectively. Although unideal voltage potential configurations were present due to hardware limitations and possible screening effects from the BGE, the PMMA ME system still performed adequately. Using the observed voltages of 400 and 3 V (i.e., $\Delta V = 397$) for Equation (4), the electric field for the separation process is then $E = 4.56$ V/mm. Using Equation (5), the t_m of CPFH is 315 s or 5.25 min. The authors believe this model could be improved upon for cross-shaped ME systems, as the traditional capillary parallel-plate model neglects the impact of the cross-section of the microchip and balance voltage potentials applied to the SA and WA wells during the separation process. The following section will propose an alternative (and we believe enhanced) method to analyze t_m in cross-shaped MEs that considers the observed voltage potentials applied by each electrode during the separation process. We label this as the cross-shaped lumped-element model.

3.2.3 | Cross-Shaped Lumped-Element Model

The cross-shaped lumped-element model involves configuring a cross-shaped ME system into the equivalent circuit resistor model shown in Figure 1C and solving for the voltage at the cross-section of the PMMA Microchip (V_{CS}). The method of solving for V_{CS} is feasible by the laws of superposition and a voltage division across the lumped-element model, where resistors R_{SA}, R_{SO}, R_{WA}, and R_{DR} are used to model the resistance of the various microchannels of the microchip. Since there is a voltage potential applied to the SA, SO, and WA wells during the separation process, the contribution of each voltage potential to the value of V_{CS} is given by

$$V_1 = V_{\text{SO}} \frac{R_{\text{SA}} \,||R_{\text{WA}}|| \, R_{\text{DR}}}{(R_{\text{SO}} + R_{\text{SA}} \,||R_{\text{WA}}|| \, R_{\text{DR}})}, \quad (8)$$

$$V_2 = V_{\text{SA}} \frac{R_{\text{SO}} \,||R_{\text{WA}}|| \, R_{\text{DR}}}{(R_{\text{SA}} + R_{\text{SO}} \,||R_{\text{WA}}|| \, R_{\text{DR}})}, \quad (9)$$

$$V_3 = V_{\text{WA}} \frac{R_{\text{SO}} \,||R_{\text{SA}}|| \, R_{\text{DR}}}{(R_{\text{WA}} + R_{\text{SO}} \,||R_{\text{SA}}|| \, R_{\text{DR}})}, \quad (10)$$

where the nomenclature $R_a||R_b$ denotes resistors R_a and R_b in parallel. The voltages V_{SO}, V_{SA}, and V_{WA} are the voltage contributions from the electrodes located at SO (400 V), SA (230 V), and WA (230 V) wells, respectively. Treating the DR (3 V) well as (approximately) ground, the resulting V_{CS} is then the superposition of Equations (8)–(10) as given by

$$V_{\text{CS}} = V_1 + V_2 + V_3. \quad (11)$$

The resistances labeled throughout Equations (8)–(10) are given by

$$R_i = \frac{l_i}{A_c \sigma_i}, \quad (12)$$

where l and σ are the length and the bulk conductivity, respectively, from a specified well to the cross-section of the microchip. The subscript i denotes the specific well (SA, SO, WA, or DR) for l, σ, and R. Here, A_c is the cross-sectional area of the microchannels (5620 μm^2 for this work). As the sample plug is estimated to only occupy 0.422 nL (i.e., < 0.1%) of the total volume of the l_{DR} microchannel (0.456 μL), while the remainder of this microchannel's volume is occupied by the BGE, it is assumed that the sample plug contributes negligible changes to σ_{DR} throughout the separation phase of the ME experiment. From this assumption then, $\sigma_{\text{SO}} \approx \sigma_{\text{DR}}$ in the context of measuring the resistance of the microchannel and is measured to be 3070 μS/cm (see Section C of the Supporting Information for the methodology of this work's conductivity measurements). The l_{SO} and l_{DR} to the cross-section of the PMMA chip are 6 and 81 mm, respectively. With Equation (12), the corresponding R_{SO} and R_{DR} are 3.48 and 46.9 MΩ, respectively. For the case of the σ_{SA} and σ_{WA}, the presence of the sample must be considered with regards to the computation of R_{SA} and R_{WA}. As depicted in Figure 2B, milk flows from the SA to the WA electrodes during the injection phase and remains in these reservoirs after the separation configuration is applied. Although the exact amount of milk and 1 mM cipro present within the SA and WA reservoirs are unknown, it will be approximated as the 1:4 ratio of milk sample and BGE solution found in the SA reservoir. The σ_{SA} and σ_{WA} are measured to be 4270 μS/cm. As l_{SA} and l_{WA} are 5 mm each, from Equation (12), we have $R_{\text{SA}} = R_{\text{WA}} = 2.08$ MΩ. With all the necessary resistances defined, V_1, V_2, and V_3 are computed with Equations (8)–(10) to be 90.5, 88.2, and 88.2 V, respectively. From Equation (11), V_{CS} is then 267 V.

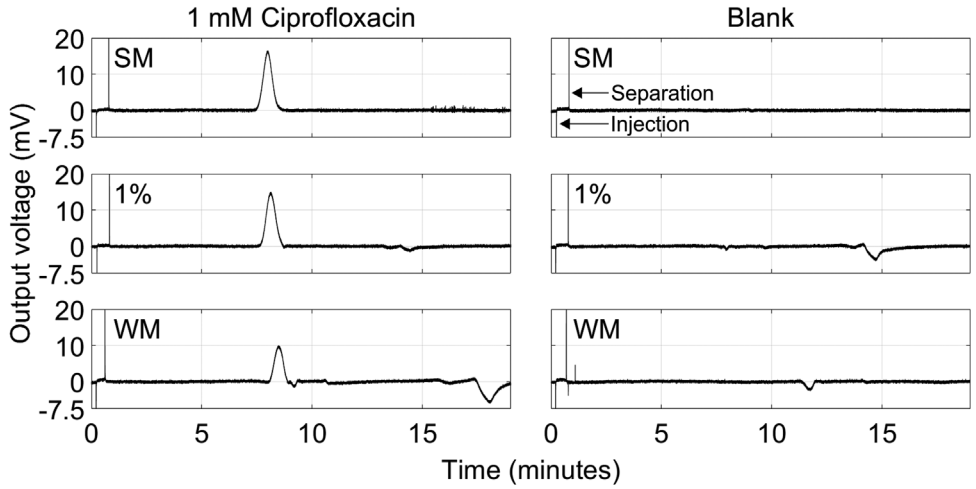

FIGURE 3 | Measurements are shown of ME experiments of 1 mM CPFH (left column) and blanks (right column) for SM (top row), 1% (middle row), and WM (bottom row). The vertical spikes present between 0 and 5 min indicate when the ME system actuated its respective injection and separation processes take place and is explicitly labeled in the SM blank plot.

Now that V_{CS} is defined, Equation (5) can be used to determine the t_m of CPFH in a cross-shaped microchip. The L for this case is the distance from the cross-section (location of V_{CS}) to the DR well ($L = 81$ mm), and the corresponding E is 3.30 V/mm. The t_m of CPFH in milk for the cross-shaped lumped-element model is 436 s, or 7.27 min, showing that the balance voltage potentials applied to SA and WA have an impact on t_m as the value differs by approximately 2 min compared to the t_m calculated for the traditional capillary parallel-plate model. Despite the differences of t_m between the traditional capillary parallel-plate model and cross-shaped microchip models, the t_m of the presented PMMA ME system for unfiltered milk is expected to be below the maximum 10-min milking time for cows [24], due to the use of SDS to improve the EOF and solubilize milk fat. The following section will showcase the results of the 1 mM CPFH signals acquired with the PMMA ME systems presented in this work and find the t_m error between the theoretical and experimental values. An evaluation and comparison of the presented ME system's performance to previously reported ME systems will also be made in the next section [25, 36].

4 | Results and Discussion

4.1 | Experimental Results

A 1 mM CPFH and blank photodiode response for each milk type (SM, 1%, and WM) is shown in Figure 3. A MATLAB curve fitting toolbox was used on all recorded photodiode responses to center the baseline signal at 0 V. The output voltage, t_m, and the full width at half maximum (FWHM) for five trials of each milk type were recorded after the data were centered to 0 V with a curve fitting algorithm. The negative quasi-Gaussian signals present after 10 min for the 1% and WM trials in Figure 3 are due to the presence of fat in these milk samples. Literature shows there is great interest in quantifying milk fat content in raw (i.e., whole) milk as its composition dictates the economic value of the milk [53, 54]. Milk fat content is affected by the diet [54, 55], health [53, 56], and welfare of the cow [54, 55]. In addition, several works describe a need for rapid diagnostic and health monitoring of cattle for optimal dairy farming [54, 56]. These findings imply that a rapid milk fat quantification system could be of practical use for the dairy industry to monitor the health of cows. However, this would require a more sophisticated version of the presented microfluidic system, which is not within the scope of this work. The detection of fat without any quantification is a redundant check for dairy applications, as a user on-farm would likely already know that the milk sample they are testing contains fat.

The output voltage, t_m, and FWHM metrics for all five trials of each corresponding milk type are shown in Figure 4. The mean and SD for each of the metrics are tabulated in Table S3. The output voltage, t_m, and FWHM of the previously reported ME system for 1 mM CPFH are extrapolated as 10.5 mV, 15.8 min, and 60 s, respectively [25]. Compared to the previous work of Bosma et al. that used filtered milk (removal of fat and proteins), the presented ME system is able to detect CPFH in unfiltered milk with no sample pretreatment—such as centrifugation—typically seen in literature [2, 25]. The improvement of the mean output voltage for the SM, 1%, and WM types is 1.54, 1.37, and 1.15 times greater, respectively, than the previously reported work [25, 36]. The presented system's t_m for unfiltered milk (mean of all 15 trials) is two times faster than the previously reported system [25, 36] and within the 10 min associated with milking a cow [24]. We are able to achieve this fast analysis time at separation voltages below 500 V because of the improvement to the EOF of the PMMA ME system from the integration of SDS-based BGE. The FWHM of the CPFH signal (mean of all 15 trials) of the presented ME system is approximately two times narrower than the previously reported system [25, 36]. This is performed for milk samples that have no pretreatment because of our use of SDS as the primary constituent within the BGE, allowing for the solubilization of milk fat [33, 34]. The linearity and estimated limit of detection of the presented ME system (12 ppm) are reported in Section E of the Supporting Information and based on the nominal response curve shown in Figure S2. With the integration of high-sensitivity sensing systems [57], this limit of detection could

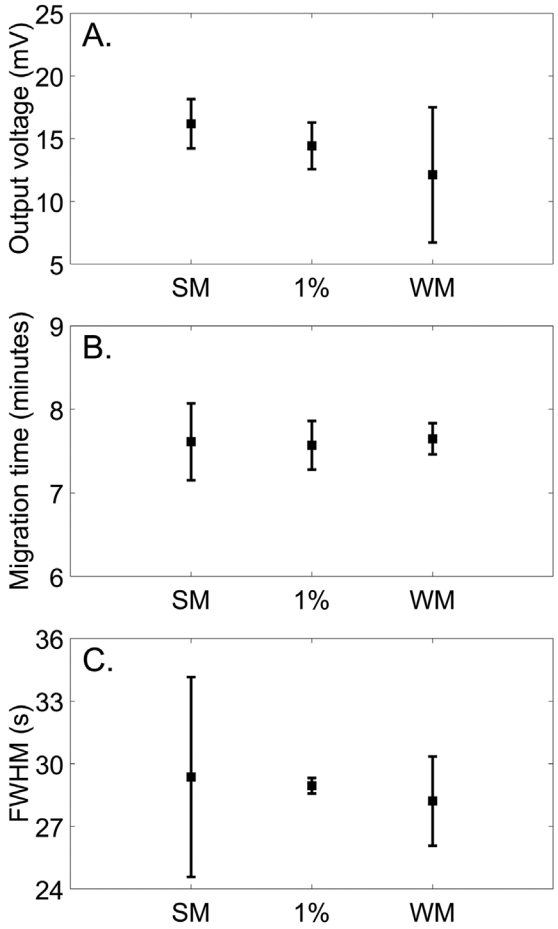

FIGURE 4 | (A) The mean and SD values of the output voltage measured for the fluorescence signal of 1 mM CPFH in unfiltered milk. (B) The mean and SD values for the t_m of 1 mM CPFH in unfiltered milk. (C) The mean and SD values for the FWHM of the 1 mM CPFH signal in unfiltered milk. Each of these metrics was calculated using five trials recorded for 1 mM CPFH in SM, 1%, and WM after it has been processed with a MATLAB curve fitting toolbox.

potentially be brought below the 0.1 ppm target of the European Union [58].

4.2 | Migration Time Differences Between Models and Experiment

As described in respective Subsections 3.2.2 and 3.2.3, a theoretical t_m value was calculated for the capillary parallel-plate model and cross-shaped lumped-element model. The theoretical t_m error (err_{mt}) for this work is quantified as

$$err_{mt} = 100\left|1 - \frac{t_{m,E}}{t_{m,T}}\right|, \tag{13}$$

where $t_{m,E}$ and $t_{m,T}$ are the experimental and theoretical t_m, respectively. For $t_{m,E}$ the mean t_m for all fifteen 1 mM CPFH trials reported in this work is 7.61 min. The $t_{m,T}$ values are the theoretical t_m values calculated for the traditional capillary parallel-plate model and cross-shaped lumped-element model, which are 5.25 and 7.27 min, respectively. Equation (13) yields an err_{mt} of 45.0% for the traditional capillary parallel-plate model and 4.68% for the cross-shaped lumped-element model. As the err_{mt} for the introduced cross-shaped lumped-element model is approximately one order of magnitude less than the traditional capillary parallel-plate model, the use of the cross-shaped lumped-element model is deemed a favorable alternative method to quantify E and the corresponding t_m in a cross-shaped ME system. A summary of the presented system's improvements to the previously published dairy ME system [25] and err_{mt} are shown in Table 1.

TABLE 1 | Tabulation of the presented system's improvements toward the output voltage, t_m, and FWHM of 1 mM CPFH in unfiltered milk over its previous iteration (rows 1–3) [25, 36]. The calculated err_{mt} between the traditional capillary parallel-plate model and cross-shaped capillary models is shown (Rows 4 and 5).

Parameter	Milk		
	SM	1%	WM
Output voltage	1.54	1.37	1.15
t_m		2.07	
FWHM		2.09	
Traditional CE err_{mt}		45.0%	
Cross-shaped err_{mt}		4.68%	

5 | Concluding Remarks

The need for adequately fast and safe (low voltage) antibiotic detection technologies is pivotal for the development of portable on-farm sensors. At the same time, a robust biosensor should be able to operate on unfiltered milk. This work described a low-voltage (< 500 V) cross-shaped PMMA ME system capable of detecting CPFH within milk under the maximum time necessary to milk a cow (10 min). The ME system presented requires no filtration, centrifugation, or chemical pretreatment of milk samples prior to ME measurements and performed better in all accounts (output voltage, migration time, and FWHM) than previous ME systems in literature used to detect CPFH in milk [21, 31]. The PMMA ME system was also found to be capable of detecting milk fat but requires further optimization to be able to reliably quantify and separate milk fat. A lumped circuit model of a cross-shaped microchip as an alternative method to determine the voltage at the injection-separation microchannel cross section for computations of the expected migration time of an analyte was introduced in this work. To the best of the authors' knowledge, this is the first reported account of a PMMA ME system capable of detecting CPFH in unfiltered milk. This work serves as an early prototype toward the overarching goal of on-farm use.

Acknowledgments

The authors respectfully acknowledge that the University of British Columbia's Okanagan campus is on the traditional, ancestral, and unceded territory of the Syilx Okanagan Nation. The authors would like to thank Seth Lowry for technical assistance. Dr. Christopher Collier would like to acknowledge research funding through the Natural

Sciences and Engineering Research Council of Canada NSERC Discovery Grant program (RGPIN-2023-04202) and NSERC Alliance Grant program (ALLRP 570519-2021).

Conflicts of Interest

This work was funded through Natural Sciences and Engineering Research Council of Canada (NSERC) through an NSERC Alliance Grant (number: ALLRP 570519-2021). This is a grant that involves an industry partner Agrisan Specialty Chemical and Pharmaceutical (which is a subsidiary of CG Wellington). Larry Wood (CG Wellington) and Dr. Khalid Moomand (Agrisan Specialty Chemical and Pharmaceutical) have had input to the manuscript and are co-authors. However, there is no direct financial conflict of interest with the work.

Data Availability Statement

The data that support the findings of this study are available upon reasonable request.

References

1. A. Manz, N. Graber, and H. M. Widmer, "Miniaturized Total Chemical Analysis Systems: A Novel Concept for Chemical Sensing," *Sensors and Actuators B: Chemical* 1 (1990): 244–248.

2. L. Ferey and N. Delaunay, "Food Analysis on Electrophoretic Microchips," *Separation and Purification Reviews* 45 (2016): 193–226.

3. A. Wuethrich and J. P. Quirino, "A Decade of Microchip Electrophoresis for Clinical Diagnostics—A Review of 2008–2017," *Analytica Chimica Acta* 1045 (2019): 42–66.

4. X. Ou, P. Chen, X. Huang, S. Li, and B. Liu, "Microfluidic Chip Electrophoresis for Biochemical Analysis," *Journal of Separation Science* 43 (2020): 258–270.

5. Y. Guo, X. Zhang, H. Zhang, et al., "Application of Microfluidic Technologies in Forensic Analysis," *Electrophoresis* 44 (2023): 1725–1743.

6. S. B. Lucas, L. M. Duarte, K. C. A. Rezende, and W. K. T. Coltro, "Nitrite Determination in Environmental Water Samples Using Microchip Electrophoresis Coupled With Amperometric Detection," *Micromachines* 13 (2022): 1–12.

7. P. Troška, E. Poboży, Z. Némethová, and M. Masár, "Determination of Commonly Used Excipients in Pharmaceutical Preparations by Microchip Electrophoresis With Conductivity Detection," *Chromatographia* 82 (2019): 741–748.

8. M. Masci, C. Zoani, T. Nevigato, et al., "Authenticity Assessment of Dairy Products by Capillary Electrophoresis," *Electrophoresis* 43 (2022): 340–354.

9. B. J. Kirby and E. F. Hasselbrink Jr., "Zeta Potential of Microfluidic Substrates: 2. Data for Polymers," *Electrophoresis* 25 (2004): 203–213.

10. G. Azadi and A. Tripathi, "Surfactant-Induced Electroosmotic Flow in Microfluidic Capillaries," *Electrophoresis* 33 (2012): 2094–2101.

11. S. Hosseini, F. Ibrahim, I. Djordjevic, and L. H. Koole, "Recent Advances in Surface Functionalization Techniques on Polymethacrylate Materials for Optical Biosensor Applications," *Analyst* 139 (2014): 2933–2943.

12. T. T. Shih, I. H. Hsu, J. F. Wu, C. H. Lin, and Y. C. Sun, "Development of Chip-Based Photocatalyst-Assisted Reduction Device to Couple High Performance Liquid Chromatography and Inductively Coupled Plasma-Mass Spectrometry for Determination of Inorganic Selenium Species," *Journal of Chromatography A* 1304 (2013): 101–108.

13. C. Long, B. Deng, S. Sun, and S. Meng, "Simultaneous Determination of Chlortetracycline, Ampicillin and Sarafloxacin in Milk Using Capillary Electrophoresis With Electrochemiluminescence Detection," *Food Additives & Contaminants* 34 (2017): 24–31.

14. P. Gutiérrez, S. E. Godoy, S. Torres, et al., "Improved Antibiotic Detection in Raw Milk Using Machine Learning Tools Over the Absorption Spectra of a Problem-Specific Nanobiosensor," *Sensors* 20 (2020): 1–13.

15. J. F. Alves, G. H. Paula, R. C. F. Silva, et al., "Residues of Antibiotics in Milk: Persistence and Quality Interference," *Canadian Journal of Animal Science* 100 (2020): 93–101.

16. T. T. Anika, Z. A. Noman, R. A. Ferdous, et al., "Time Dependent Screening of Antibiotic Residues in Milk of Antibiotics Treated Cows," *Journal of Advanced Veterinary and Animal Research* 6 (2019): 516–520.

17. C. Manyi-Loh, S. Mamphweli, E. Meyer, and A. Okoh, "Antibiotic Use in Agriculture and Its Consequential Resistance in Environmental Sources: Potential Public Health Implications," *Molecules* 23 (2018): 1–48.

18. H. El Kojok, N. El Darra, M. Khalil, et al., "Fluorescence Polarization Assay to Detect the Presence of Traces of Ciprofloxacin," *Scientific Reports* 10 (2020): 1–6.

19. S. S. Nielsen, D. J. Bicout, P. Calistri, et al., "Assessment of Animal Diseases Caused by Bacteria Resistant to Antimicrobials: Cattle," *EFSA Journal* 19 (2021): 6955–6989.

20. J. M. Mitchell, M. W. Griffiths, S. A. Mcewen, W. B. Mcnab, and A. J. Yee, "Antimicrobial Drug Residues in Milk and Meat: Causes, Concerns, Prevalence, Regulations, Tests, and Test Performance," *Journal of Food Protection* 61 (1998): 742–756.

21. J. Peris-Vicente, E. Peris-García, J. Albiol-Chiva, et al., "Liquid Chromatography, a Valuable Tool in the Determination of Antibiotics in Biological, Food and Environmental Samples," *Microchemical Journal* 177 (2022): 1–16.

22. C. Vercelli, M. Amadori, G. Gambino, and G. Re, "A Review on the Most Frequently Used Methods to Detect Antibiotic Residues in Bovine Raw Milk," *International Dairy Journal* 144 (2023): 1–12.

23. T. Elliot, B. Goldstein, and S. Charlebois, "Over 6 Billion Liters of Canadian Milk Wasted Since 2012," *Ecological Economics* 227 (2025): 1–4, https://doi.org/10.1016/j.ecolecon.2024.108413.

24. P. Kliś, D. Piwczyński, A. Sawa, and B. Sitkowska, "Prediction of Lactational Milk Yield of Cows Based on Data Recorded by AMS During the Periparturient Period," *Animals* 11 (2021): 1–11.

25. R. Bosma, J. Devasagayam, A. Singh, and C. M. Collier, "Microchip Capillary Electrophoresis Dairy Device Using Fluorescence Spectroscopy for Detection of Ciprofloxacin in Milk Samples," *Scientific Reports* 10 (2020): 1–8.

26. R. H. O. Montes, M. C. Marra, M. M. Rodrigues, E. M. Richter, and R. A. A. Muñoz, "Fast Determination of Ciprofloxacin by Batch Injection Analysis With Amperometric Detection and Capillary Electrophoresis With Capacitively Coupled Contactless Conductivity Detection," *Electroanalysis* 26 (2014): 432–438.

27. F. Trimboli, V. M. Morittu, C. Cicino, C. Palmieri, and D. Britti, "Rapid Capillary Electrophoresis Approach for the Quantification of Ewe Milk Adulteration With Cow Milk," *Journal of Chromatography A* 1519 (2017): 131–136.

28. K. Ansari, J. Y. S. Ying, P. C. Hauser, N. F. de Rooij, and I. Rodriguez, "A Portable Lab-on-a-Chip Instrument Based on MCE With Dual Top–Bottom Capacitive Coupled Contactless Conductivity Detector in Replaceable Cell Cartridge," *Electrophoresis* 34 (2013): 1390–1399.

29. S. Zhao, X. Li, and Y. M. Liu, "Integrated Microfluidic System With Chemiluminescence Detection for Single Cell Analysis After Intracellular Labeling," *Analytical Chemistry* 81 (2009): 3873–3878.

30. M. Castaño-Álvarez, A. Fernández-la-Villa, M. T. Fernández-Abedul, and A. Costa-García, "MCE-Electrochemical Detection for Following Interactions of ssDNA and dsDNA With Methylene Blue," *Electrophoresis* 30 (2009): 1943–1948.

31. M. Piñero, R. Garrido-Delgado, R. Bauza, L. Arce, and M. Valcárcel, "Easy Sample Treatment for the Determination of Enrofloxacin and Ciprofloxacin Residues in Raw Bovine Milk by Capillary Electrophoresis," *Electrophoresis* 33 (2012): 2978–2986.

32. L. Vera-Candioti, A. C. Olivieri, and H. C. Goicoechea, "Development of a Novel Strategy for Preconcentration of Antibiotic Residues in Milk and Their Quantitation by Capillary Electrophoresis," *Talanta* 82 (2010): 213–221.

33. V. Fritz, P. Martirosian, J. Machann, R. Daniels, and F. Schick, "A Comparison of Emulsifiers for the Formation of Oil-in-Water Emulsions: Stability of the Emulsions Within 9 h After Production and MR Signal Properties," *Magnetic Resonance Materials in Physics Biology and Medicine* 35 (2022): 401–410.

34. J. Juan-Colás, L. Dresser, K. Morris, et al., "The Mechanism of Vesicle Solubilization by the Detergent Sodium Dodecyl Sulfate," *Langmuir* 36 (2020): 11499–11507.

35. A. M. Khan and S. S. Shah, "pH Induced Partitioning and Interactions of Ciprofloxacin Hydrochloride With Anionic Surfactant Sodium Dodecyl Sulfate Using Ultraviolet and Fourier Transformed Infrared Spectroscopy Study," *Journal of Dispersion Science and Technology* 30 (2009): 1247–1254.

36. R. Bosma, J. Devasagayam, R. Eswar, I. F. Albuquerque, and C. M. Collier, "Voltage Control for Microchip Capillary Electrophoresis Analyses," *Electrophoresis* 41 (2020): 1961–1968.

37. C. A. Lelis, D. Galvan, L. Tessaro, J. C. de Andrade, Y. S. Mutz, and C. A. Conte-Junior, "Fluorescence Spectroscopy in Tandem With Chemometric Tools Applied to Milk Quality Control," *Journal of Food Composition and Analysis* 109 (2022): 1–10.

38. M. H. Ahmad, A. Sahar, and B. Hitzmann, "Fluorescence Spectroscopy for the Monitoring of Food Processes," in *Measurement, Modeling and Automation in Advanced Food Processing*, ed. B Hitzmann (Springer, 2017), 121–151.

39. L. Zhou, N. Gan, Y. Zhou, T. Li, Y. Cao, and Y. Chen, "A Label-Free and Universal Platform for Antibiotics Detection Based on Microchip Electrophoresis Using Aptamer Probes," *Talanta* 167 (2017): 544–549.

40. X. Yang, J. Zhao, S. Chen, Y. Huang, and S. Zhaok, "An Ultrasensitive Microchip Electrophoresis Chemiluminescence Assay Platform for Detection of Trace Biomolecules," *Journal of Chromatography A* 1613 (2020): 1–6.

41. E. Guihen, "Recent Advances in Miniaturization—The Role of Microchip Electrophoresis in Clinical Analysis," *Electrophoresis* 35 (2014): 138–146.

42. A. Gastélum-Barrios, G. M. Soto-Zarazúa, A. Escamilla-García, M. Toledano-Ayala, G. Macías-Bobadilla, and D. Jauregui-Vazquez, "Optical Methods Based on Ultraviolet, Visible, and Near-Infrared Spectra to Estimate Fat and Protein in Raw Milk: A Review," *Sensors* 20 (2020): 1–16.

43. Y. Yang, Y. Chen, H. Tang, N. Zong, and X. Jiang, "Microfluidics for Biomedical Analysis," *Small Methods* 4 (2020): 1–30.

44. V. Vaishampayan, A. Kapoor, and S. P. Gumfekar, "Enhancement in the Limit of Detection of Lab-on-Chip Microfluidic Devices Using Functional Nanomaterials," *Canadian Journal of Chemical Engineering* 101 (2023): 5208–5221.

45. Y. Bao, A. W. Lantz, J. A. Crank, J. Huang, and D. W. Armstrong, "The Use of Cationic Surfactants and Ionic Liquids in the Detection of Microbial Contamination by Capillary Electrophoresis," *Electrophoresis* 29 (2008): 2587–2592.

46. M. Novotný, F. Opekar, I. Jelínek, and K. Štulík, "Improved Dual Photometric-Contactless Conductometric Detector for Capillary Electrophoresis," *Analytica Chimica Acta* 525 (2004): 17–21.

47. L. Kartsova and A. Maliushevska, "Determination of Amino Acids and Peptides Without Their Pre-Column Derivatization by Capillary Electrophoresis With Ultraviolet and Contactless Conductivity Detection. An Overview," *Journal of Separation Science* 47 (2024): 1–21.

48. C. S. Henry, "Microchip Capillary Electrophoresis: An Introduction," in *Microchip Capillary Electrophoresis: Methods and Protocols*, ed. C. S. Henry (Humana Press, 2006), 93–113.

49. S. Hassan, "Microchip Electrophoresis," *Encyclopedia* 1 (2020): 30–41.

50. S. D. Noblitt and C. S. Henry. "Overcoming Challenges in Using Microchip Electrophoresis for Extended Monitoring Applications," in *Capillary Electrophoresis and Microchip Capillary Electrophoresis*, ed. C. D. García, K. Y. Chumbimuni-Torres, and E. Carrilho (John Wiley & Sons, Inc., 2013), 177–200.

51. H. Whatley. "Basic Principles and Modes of Capillary Electrophoresis," in *Clinical and Forensic Applications of Capillary Electrophoresis*, ed. J. R. Petersen, A. A. Mohammad (Humana Press, 2001), 21–58.

52. J. H. Masliyah and S. Bhattacharjee. "Electric Double Layer," in *Electrokinetic and Colloid Transport Phenomena*, ed. J. H. Masliyah, and S. Bhattacharjee (John Wiley & Sons, Inc., 2006), 116–123.

53. H. Z. Sun, G. Plastow, and L. L. Guan, "Invited Review: Advances and Challenges in Application of Feedomics to Improve Dairy Cow Production and Health," *Journal of Dairy Science* 102 (2019): 5853–5870.

54. B. Aernouts, E. Polshin, J. Lammertyn, and W. Saeys, "Visible and Near-Infrared Spectroscopic Analysis of Raw Milk for Cow Health Monitoring: Reflectance or Transmittance?" *Journal of Dairy Science* 94 (2011): 5315–5329.

55. A. Razzaghi, M. H. Ghaffari, and D. E. Rico, "The Impact of Environmental and Nutritional Stresses on Milk Fat Synthesis in Dairy Cows," *Domestic Animal Endocrinology* 83 (2023): 1–9.

56. A. Benedet, C. L. Manuelian, A. Zidi, M. Penasa, and M. De Marchi, "Invited Review: B-Hydroxybutyrate Concentration in Blood and Milk and Its Associations With Cow Performance," *Animal* 13 (2019): 1676–1689.

57. J. Devasagayam, C. A. Leclerc, R. Bosma, L. Wood, and C. M. Collier, "Lock-in Amplifier Dairy Sensor for Detection of Ciprofloxacin," *IEEE Access* 11 (2023): 41697–41707.

58. J. M. Barosso, "Commission Regulation (EU) No. 37/2010 on Pharmacologically Active Substances and Their Classification Regarding Maximum Residue Limits in Foodstuffs of Animal Origin," *OJEU* 15 (2010): 1–72.

Supporting Information

Additional supporting information can be found online in the Supporting Information section.